HHS Public Access

Author manuscript

Sens Biosensing Res. Author manuscript; available in PMC 2021 March 30.

Published in final edited form as:

Sens Biosensing Res. 2021 February ; 31: . doi:10.1016/j.sbsr.2020.100394.

Hydrosulfide-selective ChemFETs for aqueous H_2S/HS^- measurement

Tobias J. Sherbow, **Grace M. Kuhl**, **Grace A. Lindquist**, **Jordan D. Levine**, **Michael D. Pluth***, **Darren W. Johnson***, **Sean A. Fontenot***

Department of Chemistry and Biochemistry, Materials Science Institute, University of Oregon, Eugene, Oregon 97403, United States

Abstract

We have prepared and characterized hydrosulfide-selective ChemFET devices based on a nitrile butadiene rubber membrane containing tetraoctylammonium nitrate as a chemical recognition element that is applied to commercially available field-effect transistors. The sensors have fast (120 s) reversible responses, selectivity over other biologically relevant thiol-containing species, detection limits of 8 mM, and a detection range from approximately 5 to 500 mM. Sensitivities are shown to be 53 mV per decade at pH 8. Use of this compact, benchtop sensor platform requires little training – only the ability to measure DC voltage, which can be accomplished with a conventional multimeter or a simple analog data acquisition device paired with a personal computer. To the best of our knowledge, this report describes the first example of direct potentiometric measurement of the hydrosulfide ion in water.

1. Introduction

Hydrogen sulfide (H_2S) is an important analytical target for a diverse set of sensing applications including environmental sensing, biomedical sciences, and petroleum and natural gas industries. H_2S is produced during the decomposition of organic matter and is naturally present in ponds, swamps, landfills and sewage systems. H_2S is also found in natural gas and crude oil and is considered a contaminant in refined petroleum and gas products [1]. Due to the toxicity and environmental prevalence of H_2S (from both natural and unnatural sources) further development of environmental H_2S sensing methods is needed [2]. H_2S has also been established as an important small molecule biological mediator and is associated with different physiological conditions including diabetes, hypertension, neurodegeneration, and heart failure [3–8].

*Corresponding authors. pluth@uoregon.edu (M.D. Pluth), dwj@uoregon.edu (D.W. Johnson), sfonteno@uoregon.edu (S.A. Fontenot).

Declaration of Competing Interest

The authors declare that they have no known competing financial interests or personal relationships that could have appeared to influence the work reported in this paper.

Appendix A. Supplementary data

Supplementary data to this article can be found online at https://doi.org/10.1016/j.sbsr.2020.100394.

Critical challenges remain for current aqueous H_2S measurement methods that limit their utility in different sensing environments. Reaction-based analytical methods, such as monobromobimane (mBB) sulfide trapping, feature excellent detection limits (below 200 nM) yet typically require long reaction/measurement times and extensive sample preparation [9–11]. Alternatively, amperometric H_2S measurement methods exist, and devices that support these are available, with primary suppliers being Unisense (Aarhus, Denmark) and World Precision Instruments (Sarasota FL, USA). These also offer excellent detection limits (5–100 nM), however, they have comparatively short lifetimes, and may in some cases show responses to other sulfur-containing species such as cysteine, glutathione, sulfur dioxide, dimethyl sulfoxide and alkyl thiols, and require highly sensitive electronics to resolve very small signal currents, which can be as low as 10^{-13} Amperes. For many environmental samples, gas chromatography (GC) methods are adequate, but such methods are less convenient and are much more resource intensive than sensor-based methods [12,13]. Overall, there are opportunities to develop new technologies and methods for measuring H_2S in a variety of physiologically and environmentally relevant applications and sample matrices. The diversity of sensing environments and associated detection ranges necessitate new chemical tools for H_2S detection and measurement. Potentiometric methods in particular have been poorly represented in environmental, petrochemical, and biological application spaces and provide an opportunity for continued development [12].

H_2S has a pK_a near 7 and is primarily present as its conjugate base, hydrosulfide (HS^-), at physiological temperature and pH. The sulfide dianion (S^{2-}) does not exist under physiologically relevant conditions [13]. As an ion, HS^- is susceptible to direct detection by potentiometric methods, which are rarely considered for aqueous H_2S/HS^- measurement [14]. Herein, we present a new method for direct measurement of aqueous HS^- using chemically sensitive field effect transistors (ChemFETs). Examples of ChemFETs, OFETs, and other FET-based sensors for hydrogen sulfide exist for the gas phase [15–18]; yet there are not, to our knowledge, examples of potentiometric methods, FET-based or otherwise, for direct measurement of the hydrosulfide anion in water.

ChemFETs are often described as metal-oxide-semiconductor field effect transistors (MOSFETs), which have had the gate electrode separated from the gate oxide and the now-exposed gate oxide modified to be selective for specific chemical species [19]. Often this modification involves the application of a chemically selective membrane to the gate oxide. Some benefits of ChemFETs include their quick response times, minimal sample processing requirements and a library of well-established methods for modification of surfaces and of the gate oxide interface with chemical recognition agents [20–22].

The ChemFETs described in this work feature a polymer membrane formulated with a non-covalently associated HS^- ionophore. They provide detection of HS^- in real-time with selectivity over sulfur-containing compounds including cysteine and glutathione, which are common interferants in H_2S measurements. These devices enable measurement methods which require minimal sample preparation (simple pH adjustment) to ensure that HS^- is present and that H_2S is not lost due to degassing from the solution that is being measured.

2. ChemFET overview

ChemFETs function according to similar principles as MOSFETs. In short, the threshold voltage of an enhancement mode ChemFET $\left(V_{th}^{CFET}\right)$ is related to the activity of chemical species present in solution between the gate electrode (which may be a reference or pseudo-reference electrode) and the gate oxide. V_{th}^{CFET} is defined as the minimum potential between the ChemFET gate electrode and source required to open the conducting channel between the source and drain. V_{th}^{CFET} is the sum of threshold voltage of the underlying FET $\left(V_{th}^{CFET}\right)$ and the combined contributions from the rest the chemical cell, V_{cell}.

$$V_{th}^{CFET} = V_{th}^{FET} + V_{cell} \tag{1}$$

V_{th}^{FET} is determined by the materials and geometry of the FET portion of the device and is independent of most environmental variables. Therefore, V_{th}^{FET} is effectively constant, and a change in V_{th}^{CFET} is the result only of a corresponding change in V_{cell}.

Physically, the cell includes the environment between the gate oxide, the chemically selective material, the sample environment, and the reference electrode (Fig. 1). This environment includes several chemical and material interfaces each with an associated junction potential. Fortunately, not all of these potentials need to be considered or even known. When ideally constructed, the junction potential of the chemically selective material is the only variable, and therefore a change in V_{cell} and the corresponding change in V_{th}^{CFET} is due solely to the activity of the target ion. This requires, at minimum, a reference electrode that is insensitive to changes in target ion concentration and a chemically selective material that responds primarily to the desired analytical target.

In practice, perfect selectivity is elusive and the relationship between V_{cell}, the activities of the analytical target (A), and the activity of a potential interferent (B) can be described by the Nikolsky-Eisenmann equation [20,23].

$$V_{cell} = V_{cons} + \frac{2.303\,RT}{z_A F} log\left(a_A + K_{A,B}\, a_B^{z_A/z_B}\right) \tag{2}$$

V_{cons} represents the sum of all the constant interfacial potentials in the cell, a_A and a_B are the activities of A and B, and z_A and z_B are the corresponding ionic charges of A and B. R and F are the ideal gas constant and Faraday constant, respectively, and T is temperature. Finally, $K_{A,B}$ is the experimentally determined selectivity coefficient representing the ability of the ChemFET to distinguish between A and B. Since the only variables affecting V_{cell} are a_A and a_B, ΔV_{th}^{CFET} depends entirely on ΔV_{cell} (again, V_{th}^{FET} is constant). What remains then is to transduce V_{th}^{CFET} into the measurement signal.

Note that in the absence of an interfering ion, a_B, eq. 2 reduces to a form of the Nernst equation which, when T = 25 °C and when z_A is +1 or −1, is

$$V_{cell} = 0.059\, V\, log_{10} a_A \quad (3)$$

According to Eq. 3, 59 mV represents the maximum possible change in V_{cell} for each decade change in the activity of an ionic species having a charge of +1 or −1. This is referred to as the Nernstian limit.

3. Experimental

3.1. Reagents

Sodium hydrosulfide (NaSH) was purchased from Strem Chemicals and stored in a nitrogen filled glovebox. All other reagents and solvents were purchased from Sigma-Aldrich or Tokyo Chemical Industry (TCI) and used as received. Note: NaSH and ammonium sulfide are toxic and will liberate H_2S when exposed to water. All handling of these chemicals should be performed in a glove box or fume hood in order to prevent personal exposure. A zinc acetate quench solution should be available at all times [24,25]. Additionally, a personal H_2S meter should be used to monitor potential exposure to H_2S whenever reagents and solutions are removed from the glove box.

3.2. Membrane and sensor preparation

Nitrile butadiene rubber (NBR) was obtained from Zeon Chemicals (Nipol DN401LL). FETs with unmodified gate oxides were purchased from Winsense™ (www.winsense.co.th, WIPS-C). These pre-functionalized FETs were cleaned immediately prior to modification by soaking in 30% H_2O_2 for 20 min followed by rinsing with DI water and then with ethanol. Chemically selective membranes of approximately 150 μm thickness were applied to the gate oxide by drop casting. Sulfide-sensitive membranes were made as follows: 0.1 wt% tetraoctylammonium (TOA) nitrate and 5 wt% NBR were dissolved in anisole. These solutions were drop cast onto the gate oxide surface and then dried at ambient temperature for 15 min followed by 80 °C for 12 h. After cooling to ambient temperature and then soaking in 1 M sodium nitrate solutions for approximately one hour, the sensors were ready for use.

3.3. Ag/Ag_2S reference electrode fabrication

Ag/Ag_2S wires were prepared by soaking silver wire (99.9%, 0.5 mm dia) in 5% ammonium sulfide solution overnight. One end of each wire was then soldered to a 20 AWG tinned copper wire and the solder joint completely encased in Loctite Marine Epoxy (1919324). To form each electrode body, a 4 Å molecular sieve was pressed into the tapered end of a 1 mL polypropylene syringe body (Norm-Ject 4010.200v0). Agarose (2 wt%) was dissolved in warm 3 M KCl, and 0.8 mL of this solution was poured into the syringe bodies and allowed to cool. The Ag/Ag_2S wire was then inserted into the electrode body, and the wire was secured to the housing. Reference electrodes were stored in 3 M KCl overnight before their first use. Reference potentials were found to be 129–146 mV vs SCE.

3.4. Electrode surface characterization

Elemental composition and surface morphology were determined by scanning electron microscopy energy dispersive X-ray spectroscopy (SEM-EDS) using a ThermoFisher Helios Hydra Plasma FIB. Images were collected with an accelerating voltage of 10 kV. Additional elemental analysis was performed using Thermo Scientific ESCALAB 250 X-ray photoelectron spectrometry (XPS) system with an Al Kα monochromated source at 20 kV. Survey spectra were taken along with high-resolution scans of Ag 3d, S 2p, and Cl 2p. Spectra were peak fit using the Thermo Scientific Avantage 4.88 software to determine surface composition.

3.5. Potentiometric measurements

The ChemFETs were operated by a circuit that uses an instrumentation amplifier to drive the source to drain voltage (V_{DS}) of the FET at 617.5 mV and the drain current (I_D) at 99.6 μA. The circuit keeps the external reference electrode at ground while the voltage between source and ground (V_{GS}) is changed in order to maintain V_{DS} and I_D as identified above. V_{GS} is taken as the measurement signal. See supporting information for a description of the analog circuit.

The analog V_{GS} signal was recorded using a National Instruments DAQ 6009 data acquisition unit connected to a Windows™ computer and operated by a custom LabView™ program. The signal was recorded at a rate of 1 kHz. Unless otherwise noted, each measurement was taken as the average of the signal over the 120th second of the measurement period and experiments were performed with four identical (replicate) sensors and in triplicate. All sensors were paired with Ag/Ag_2S reference electrodes.

HS^- stock solutions were prepared in an oxygen-free glovebox or using Schlenk techniques to prevent oxidation. The solutions were prepared by the addition of solid NaSH to a degassed 50 mM PIPES pH 8.0 buffer solution. The PIPES buffer was prepared by dissolving 1,4-piperazinediethanesulfonic acid in DI water and adjusting the pH with analytically pure 4 M KOH. This alkaline solution was chosen to limit the protonation of HS^-, which accelerates loss of H_2S from the calibration solutions due to volatilization. Potentiometric measurements were carried out in a fume hood at ambient temperature in 50 mL polypropylene centrifuge tubes, which were kept sealed for the duration of the experiment to minimize analyte loss due to volitilization. Activity coefficients were calculated using the Davies equation. Selectivity coefficients were determined by the Fixed Interference method according to IUPAC recommendations [29]. All uncertainties are reported as Standard Error of the Mean (SEM).

4. Results and discussion

4.1. Reference electrode fabrication and characterization

ChemFETs can be used alongside conventional Ag/AgCl reference electrodes, however, due to the corrosive properties of aqueous hydrosulfide, an alternative reference electrode (RE) is required for potentiometric measurements. Ag/AgCl REs were initially used to evaluate ChemFET performance, but we observed inconsistent RE function and drift during

measurements. We hypothesized that the chloride on the Ag wire surface was being replaced with a sulfide species. This undesired reactivity at the electrode would change the junction potential of the RE, which would manifest as signal drift.

To test this hypothesis, four samples of Ag wire were exposed to different treatments: two were submerged in household bleach (sample 1 and 3) or 5% ammonium sulfide (sample 2 and 4) for 2 h. Electrodes 3 and 4 were soaked in a pH 8 NaSH solution for 8 h after being soaked in bleach and ammonium sulfide, respectively. The four electrode wires were then analyzed by scanning electron microscope coupled with electron dispersive X-ray spectroscopy (SEM-EDS) to compare the morphology and elemental composition before and after exposure to NaSH solutions. X-ray photoelectron spectroscopy (XPS) was used to confirm composition. SEM-EDS imaging (Fig. 2b) displays the morphology of each sample as well as elemental maps of the silver, chlorine, and sulfur. The elemental composition (Table S1) from sample 3 closely match those from samples 2 and 4, which would be expected to only have sulfur on the surface of the wire. Fig. 2a shows the XPS survey spectra and high resolution scans of samples 1, 2, 3 and 4. Survey spectra indicate that Ag, Cl and Na are the main elements present in sample 1 and Ag and S the main elements in samples 2, 3 and 4. All four samples show the presence of C and O from adventitious hydrocarbon present in the XPS instrument. The peaks at 368.1 eV and 374.1 eV can be assigned to the binding energy of Ag $3d^{3/2}$ and Ag $3d^{5/2}$ present from the Ag^+ in AgCl (sample 1) and Ag_2S (sample 2/3/4). High resolution scans of Cl 2p shows the presence of Cl in sample 1, minimal presence in sample 3 (0.4%), and none in samples 2 and 4. Comparison of sulfur spectra presents a significant difference between samples 2 and 3. The S 2p scan indicates the presence of Ag_2S in samples 2 and 3 at 161 eV and 162.2 eV. However, sample 3 contains peaks at 168.2 eV and 169.2 eV, revealing the presence of $Ag_2(SO_4)$ in addition to Ag_2S. Taken together, this alternative sulfur speciation on the surface of the wire may explain loss in Ag/AgCl reference electrode functionality upon exposure to NaSH solution. Critically, samples 2 and 4 are identical, indicating that the Ag_2S surface is stable to the NaSH-containing solutions. These data suggested that the Ag/AgCl would not be useable for our potentiometric measurements for HS^-, prompting us to develop an Ag_2S coated electrode that was more stable to HS^- solutions and could serve as a more robust reference electrode.

4.2. ChemFET preparation

The key feature of our HS^- selective ChemFETs is the application of a hydrosulfide-selective polymer membrane, to the silicon nitride gate oxides of commercially available pH-sensitive FETs. ChemFETs often have chemically selective membranes comprised of PVC, PDMS, and occasionally NBR among other formulations [22,26–29]. Generally, the polymers alone have limited native sensitivity to ionic targets and their sensitivity/selectivity is be imparted by incorporating chemical recognition elements (CRE) into the polymer membranes to create the interfacial chemically selective material of the device.

Tetraoctylammonium (TOA) was chosen as our CRE. Quaternary ammonium salts are perhaps most studied for anion sensing applications because they are stable cations and many are sufficiently lipophilic to remain in the polymer membranes without covalent

attachment. TOA and other quaternary ammonium salts have been incorporated into ChemFETs, ion selective electrodes, and other potentiometric sensing platforms, some of which have been shown to be functional for up to eight weeks in aqueous environments [30]. Also, quaternary alkyl ammonium salts of HS^- have been shown to associate with HS^- in particular via C–H hydrogen bonding interactions, suggesting that this ionophore might serve as a recognition agent for HS^- [31].

NBR was chosen as the polymer component of the membrane primarily because NBR membranes enable the TOA CRE to be incorporated into the material without the requirement of any plasticizers or other fillers or additives. NBR is also inert under the sample conditions and adheres to the gate oxide well enough to allow an operational lifetime of over 46 h.

4.3. Sensitivity and calibration

To obtain a measurement signal from a ChemFET, an analog circuit must be used to interface with the FET and reference electrode [32]. Hydrosulfide-selective sensors were operated in a constant current configuration in which the input voltage (V_{DS}) and drain current (I_D) are maintained constant in a feedback mode such that the gate voltage (V_{GS}), which is the potential between the reference electrode and source, is equal to the threshold voltage of the ChemFET $\left(V_{th}^{CFET}\right)$. V_{GS} is then taken as the measurement signal. For this system V_{GS} is in the range of 0.5–3 V which may be accurately measured using comparatively simple equipment such as a basic multimeter or simple data acquisition (see Supporting Information, Section 2). Potential response curves of devices functionalized with NBR and TOA are shown in Fig. 3. When TOA was not included in the NBR membrane, no hydrosulfide response was observed. Devices with membranes containing NBR and TOA have near-Nernstian sensitivities of 53 ± 2 mV per decade from 20 to 450 mM and a detection limit of 7.7 ± 0.6 mM. These results suggest that TOA is a necessary chemical recognition agent in these devices.

4.4. Response time and reversibility

Sensor responses were recorded continuously for 300 s. As shown in Fig. 4, the devices reach their equilibrium responses (having a drift of less than 1 mV per min) within 120 s except for very high concentrations (450 mM) in which the drift was as high as 5 mV per min. As a compromise between efficiency and accuracy and to limit the exposure of the FETs and reference electrodes to high concentrations of sulfide, measurement responses were generally taken as the potential of V_{GS} at 120 s. The reproducibility of three calibration experiments is shown for a single sensor by measuring varying [HS^-] in pH 8 PIPES buffer (Fig. 5). The first and last experiments were performed in order of descending hydrosulfide concentration whereas the second experiment was run in the reverse direction, showing that the single sensor maintains repeatable HS^- response characteristics.

4.5. Selectivity studies

The practicality of chemical sensors depends largely on their selectivity for their target over other chemical species. The Fixed Interference method was used to determine selectivity

coefficients for hydrosulfide ($K_{SH, X}$) over thiol-containing small molecules such as glutathione (GSH) and cysteine as well as chloride [33]. As expected, when significant interference is observed, there is a corresponding increase in the effective detection limit (EDL). In Table 1, EDL represents an effective detection limit of these devices for HS^- in the presence of 200 mM of each interferent.

These sensors show a favorable selectivity coefficient of 0.12 for hydrosulfide over chloride. Interestingly, the few supramolecular hosts that are able to bind HS^- often show similar binding constants for HS^- and Cl^-, presumably because both ions are of similar size, whereas our sensors show almost an order of magnitude preference for HS^- over Cl^- [34,35]. The higher selectivity for HS^- over Cl^- may be due, in part, to the weak CH···S hydrogen bonding interactions observed in quaternary ammonium salts with S atoms [31]. The interfering ability of cysteine is similar that of Cl^-.

5. Conclusions

We report a new FET-based sensing platform effective in measuring hydrosulfide in the presence of other sulfur-containing species. To our knowledge, this is the first reported potentiometric method for direct hydrosulfide detection in water. The sensor is comprised of a commercially available pH-sensitive ISFET, which was coated with a polymer membrane containing tetraoctylammonium nitrate. In optimized conditions, sensitivity and detection limit were found to be 53 mV per decade and 8 mM, respectively. The sensor shows a reversible response, and devices retain useful sensitivity for at least 46 operational hours. We acknowledge that this detection limit of these proof-of-concept devices is not yet sufficient for application in many applications, such as biomedical applications, but view this approach a modifiable platform for future refinement. These first-generation ChemFET devices provide a promising lead in this direction with their strong HS^- selectivity, reversible and repeatable sensing, fast response times, and selectivity over common thiol-containing interferents.

Supplementary Material

Refer to Web version on PubMed Central for supplementary material.

Acknowledgements

Research reported herein was supported by the NIH (1R21GM129590 to SAF), and the M.J. Murdock Charitable Trust (to MDP and DWJ) (201811528). This work was also supported by the Bradshaw and Holzapfel Research Professorship in Transformational Science and Mathematics to DWJ.

References

[1]. Driver L, Freedman E, Report to Congress on Hydrogen Sulfide Air Emissions Associated with the Extraction of Oil and Natural Gas, U.S. Environmental Protection Agency, Research Triangle Park, NC. Office of Air Quality Planning and Standards, 1993. Report No: EPA-453/R-93–045; 68-D2–0065.

[2]. U.S. Department of Energy, U.S. Dry Natural Gas Production. www.eia.gov/dnav/ng/hist/n9070us2m.htm (accessed October 2, 2019).

[3]. Wang R, Physiological Implications of Hydrogen Sulfide: A Whiff Exploration That Blossomed, Physiol Rev 92 (2012) 791–896, 10.1152/physrev.00017.2011. [PubMed: 22535897]

[4]. Yang G, Wu L, Jiang B, Yang W, Qi J, Cao K, et al., H_2S as a Physiologic Science 322 (2008) 587–590, 10.1126/science.1162667. [PubMed: 18948540]

[5]. Feng X, Chen Y, Zhao J, Tang C, Jiang Z, Geng B, Hydrogen sulfide from adipose tissue is a novel insulin resistance regulator, Biochem. Biophys. Res. Commun 380 (2009) 153–159, 10.1016/j.bbrc.2009.01.059. [PubMed: 19166813]

[6]. Whiteman M, Cheung NS, Zhu Y-Z, Chu SH, Siau JL, Wong BS, et al., Hydrogen sulphide: a novel inhibitor of hypochlorous acid-mediated oxidative damage in the brain? Biochem. Biophys. Res. Commun 326 (2005) 794–798, 10.1016/j.bbrc.2004.11.110. [PubMed: 15607739]

[7]. Wang R, Two's company, three's a crowd: can H2S be the third endogenous gaseous transmitter? The FASEB J 16 (2002) 1792–1798, 10.1096/fj.02-0211hyp. [PubMed: 12409322]

[8]. Wang R, The Gasotransmitter Role of Hydrogen Sulfide, Antioxid. Redox Signal 5 (2003) 493–501, 10.1089/152308603768295249. [PubMed: 13678538]

[9]. Lin VS, Chen W, Xian M, Chang CJ, Chemical probes for molecular imaging and detection of hydrogen sulfide and reactive sulfur species in biological systems, Chem. Soc. Rev 44 (2015) 4596–4618, 10.1039/C4CS00298A. [PubMed: 25474627]

[10]. Fogo JK, Popowsky M, Spectrophotometric Determination of Hydrogen Sulfide, Anal. Chem 21 (1949) 732–734, 10.1021/ac60030a028.

[11]. Montoya LA, Pearce TF, Hansen RJ, Zakharov LN, Pluth MD, Development of Selective Colorimetric Probes for Hydrogen Sulfide Based on Nucleophilic Aromatic Substitution, J. Org. Chem 78 (2013) 6550–6557, 10.1021/jo4008095. [PubMed: 23735055]

[12]. Pandey SK, Kim K-H, Tang K-T, A review of sensor-based methods for monitoring hydrogen sulfide, Trends Anal. Chem 32 (2012) 87–99, 10.1016/j.trac.2011.08.008.

[13]. a)Pandey SK, Kim K-H, A review of methods for the determination of reduced Sulfur compounds (RSCs) in air, Environ. Sci. Technol 43 (2009) 3020–3029, 10.1021/es803272f; [PubMed: 19534108] bMay PM, Batka D, Königsberger E, Rowland D, Goodbye to S2- in aqueous solution, Chem.Commun 16 (2018) 1980–1983, 10.1039/C8CC00187A.

[14]. Zdrachek E, Bakker E, Potentiometric Sensing, Anal. Chem 91 (2019) 2–26, 10.1021/acs.analchem.8b04681. [PubMed: 30335354]

[15]. Sizov AS, Trul AA, Chekusova V, Borshchev OV, Vasiliev AA, Agina EV, et al., Highly Sensitive Air-Stable Easily Processable Gas Sensors Based on Langmuir–Schaefer Monolayer Organic Field-Effect Transistors for Multiparametric H2S and NH3 Real-Time Detection, ACS Appl. Mater. Interfaces 10 (2018) 43831–43841, 10.1021/acsami.8b15427. [PubMed: 30465602]

[16]. Shivaraman MS, Detection of H2S with Pd-gate MOS field-effect transistors, J. Appl. Phys 47 (1976) 3592–3593, 10.1063/1.323162.

[17]. Lundström I, Armgarth M, Spetz A, Winquist F, Gas sensors based on catalytic metal-gate field-effect devices, Sens. Actuators 10 (1986) 399–421, 10.1016/0250-6874(86)80056-7.

[18]. Lloyd Spetz A, Unèus L, Svenningstorp H, Tobias P, Ekedahl L-G, Larsson O, et al., SiC Based Field Effect Gas Sensors for Industrial Applications, Phys. Status Solidi 185 (2001) 15–25, 10.1002/1521-396x(200105)185:1<15::aid-pssa15>3.0.co;2-7.

[19]. Bergveld P, Thirty years of ISFETOLOGY: What happened in the past 30 years and what may happen in the next 30 years, Sens. Actuators B-Chem 88 (2003) 1–20, 10.1016/S0925-4005(02)00301-5.

[20]. Kaisti M, Detection principles of biological and chemical FET sensors, Biosens. Bioelectron 98 (2017) 437–448, 10.1016/j.bios.2017.07.010. [PubMed: 28711826]

[21]. Janata J, Potentiometric Sensors, Principles of Chemical Sensors, Springer US, Boston, MA, 2009, pp. 119–199.

[22]. Iskierko Z, Noworyta K, Sharma PS, Molecular recognition by synthetic receptors: Application in field-effect transistor based chemosensing, Biosens. Bioelectron 109 (2018) 50–62, 10.1016/j.bios.2018.02.058. [PubMed: 29525669]

[23]. Bobacka J, Ivaska A, Lewenstam A, Potentiometric Ion Sensors, Chem. Rev 108 (2008) 329–351, 10.1021/cr068100w. [PubMed: 18189426]

[24]. Hughes MN, Centelles MN, Moore KP, Making and working with hydrogen sulfide: The chemistry and generation of hydrogen sulfide in vitro and its measurement in vivo: A review, Free Radic. Biol. Med 47 (2009) 1346–1353, 10.1016/j.freeradbiomed.2009.09.018. [PubMed: 19770036]

[25]. Hartle MD, Pluth MD, A practical guide to working with H^2S at the interface of chemistry and biology, Chem. Soc. Rev 45 (2016) 6108–6117, 10.1039/C6CS00212A. [PubMed: 27167579]

[26]. Ebdon L, Braven J, Frampton NC, Nitrate-selective electrodes with polymer membranes containing immobilised sensors, Analyst 115 (1990) 189–193, 10.1039/AN9901500189.

[27]. Antonisse MMG, Lugtenberg RJW, Egberink RJM, Engbersen JFJ, Reinhoudt DN, Durable nitrate-selective chemically modified field effect transistors based on new polysiloxane membranes, Anal. Chim. Acta 332 (1996) 123–129, 10.1016/0003-2670(96)00238-3.

[28]. Stauthamer WPRV, Engbersen JFJ, Verboom W, Reinhoudt DN, Influence of plasticizer on the selectivity of nitrate-sensitive CHEMFETs, Sens. Actuators B-Chem 17 (1994) 197–201, 10.1016/0925-4005(93)00870-5.

[29]. Cao A, Mescher M, Bosma D, Klootwijk JH, Sudhölter EJR, L.C.P.M.d. Smet, Ionophore-containing Siloprene membranes: direct comparison between conventional ion-selective electrodes and silicon nanowire-based field-effect transistors, anal, Chem 87 (2015) 1173–1179, 10.1021/ac504500s.

[30]. Jørgen Nielsen H, Hansen EH, New nitrate ion-selective electrodes based on quaternary ammonium compounds in nonporous polymer membranes, Anal. Chim. Acta 85 (1976) 1–16, 10.1016/S0003-2670(01)82975-5.

[31]. Hartle MD, Meininger DJ, Zakharov LN, Tonzetich ZJ, Pluth MD, NBu4SH provides a convenient source of HS^- soluble in organic solution for H2S and anion-binding research, Dalton Trans 44 (2015) 19782–19785, 10.1039/C5DT03355A. [PubMed: 26536835]

[32]. Moser N, Lande TS, Toumazou C, Georgiou P, ISFETs in CMOS and Emergent Trends in Instrumentation: A Review, IEEE Sens. J 16 (2016) 6496–6514, 10.1109/JSEN.2016.2585920.

[33]. Buck RP, Lindner E, Recommendations for Nomenclature of Ion-Selective Electrodes, Pure Appl. Chem, IUPAC1994.

[34]. Hartle MD, Hansen RJ, Tresca BW, Prakel SS, Zakharov LN, Haley MM, et al., A Synthetic Supramolecular Receptor for the Hydrosulfide Anion, Angew. Chem. Int. Ed 55 (2016) 11480–11484, 10.1002/anie.201605757.

[35]. Lau N, Zakharov LN, Pluth MD, Modular tripodal receptors for the hydrosulfide (HS^-) anion, Chem. Commun 54 (2018) 2337–2340, 10.1039/C7CC09405A.

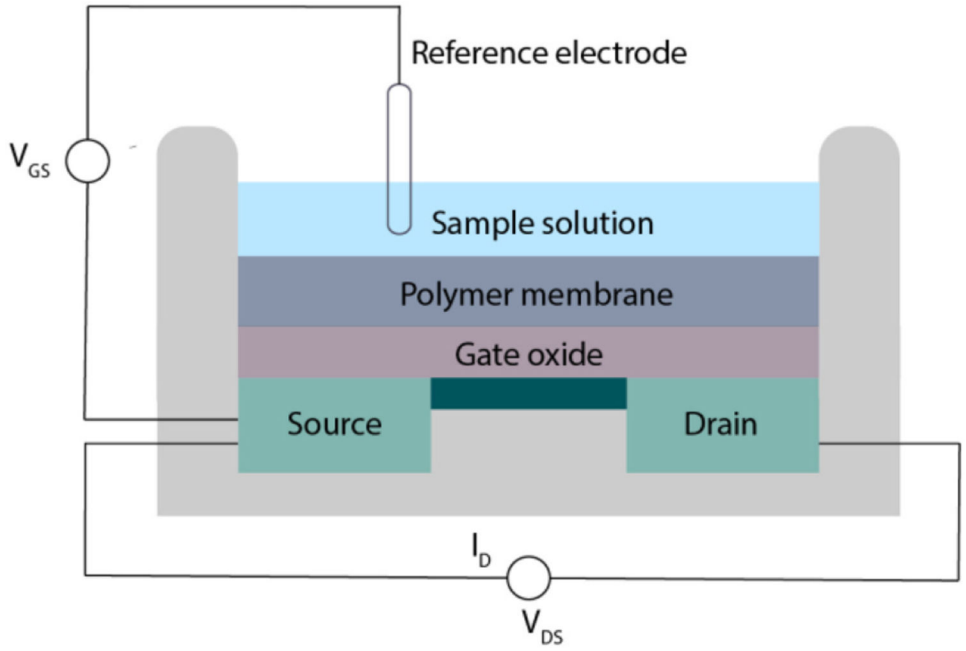

Fig. 1.

Schematic illustration of a ChemFET featuring the polymer membrane at the interface between the sample solution and the gate oxide. The operational mode of the ChemFET is such that $V_{th}^{CFET} = V_{GS}$, which is taken as the measurement signal.

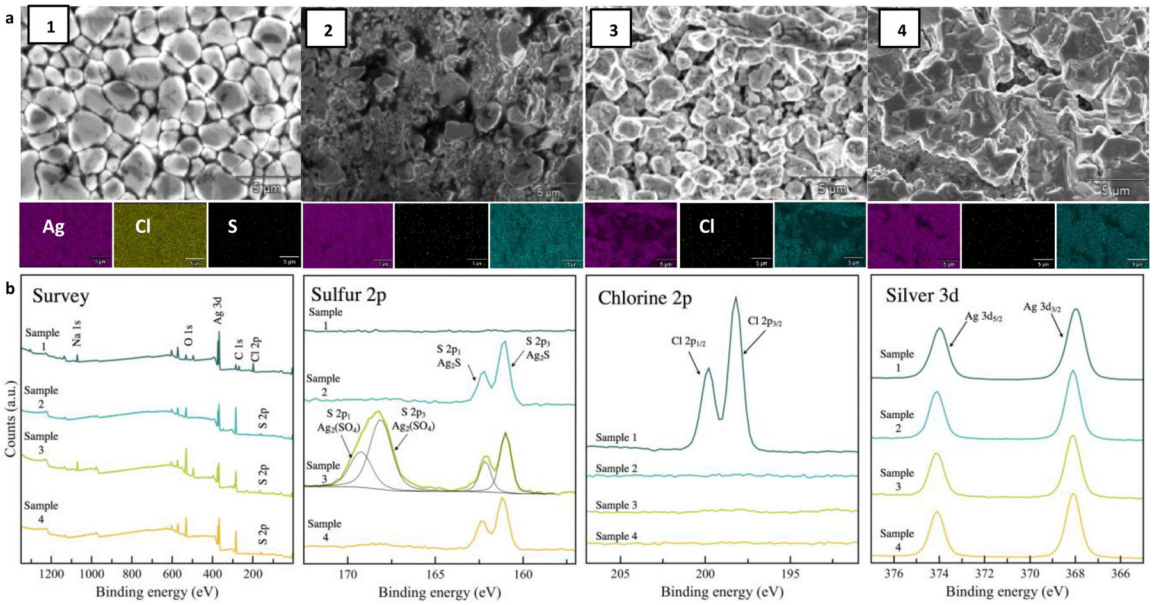

Fig. 2.

a) SEM-EDS images of Ag wire samples 1–4. 1) Control. Ag/AgCl. 2) ammonium sulfide. 3) Ag/AgCl and then NaSH. 4) Ammonium sulfide and then NaSH. b) XPS spectra of elements of interest (Cl, S, Ag) in samples 1 (blue), 2 (aqua), 3 (green) and 4 (yellow).

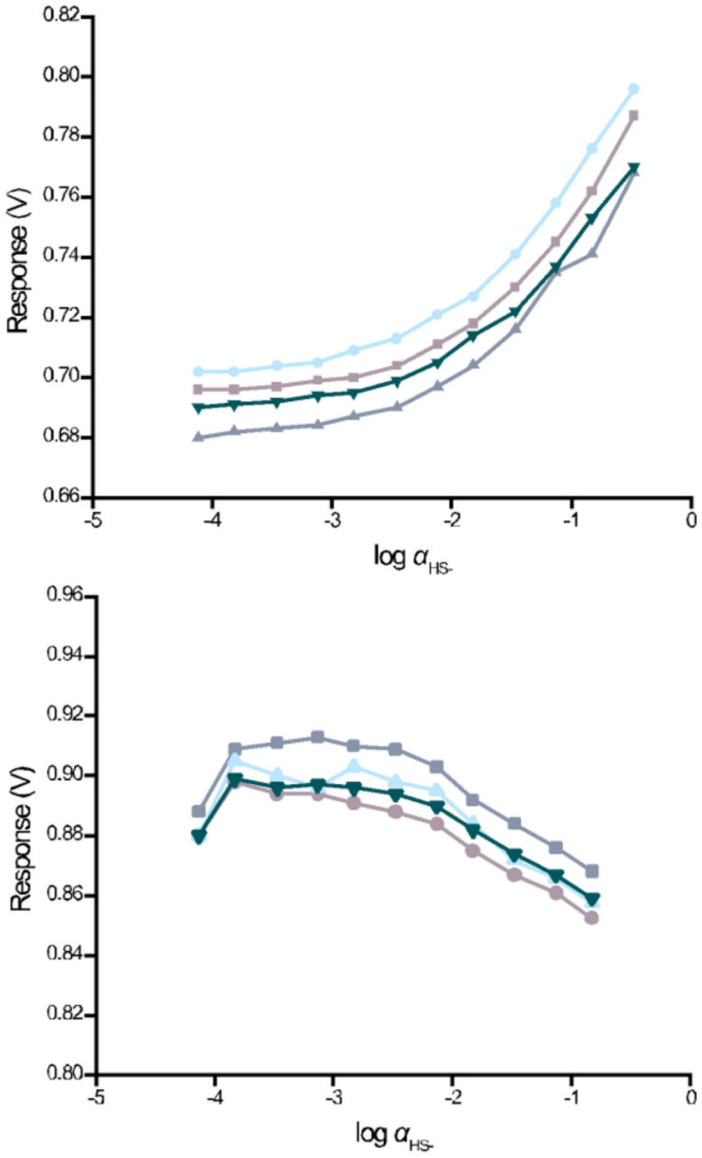

Fig. 3.

(top) Calibration runs of four identical sensors functionalized with TOA/NBR membrane showing a linear response to hydrosulfide activity (aHS^-) in 50 mM PIPES buffer from approximately 10 to 450 mM HS^-. (bottom) The responses of four identical are shown.

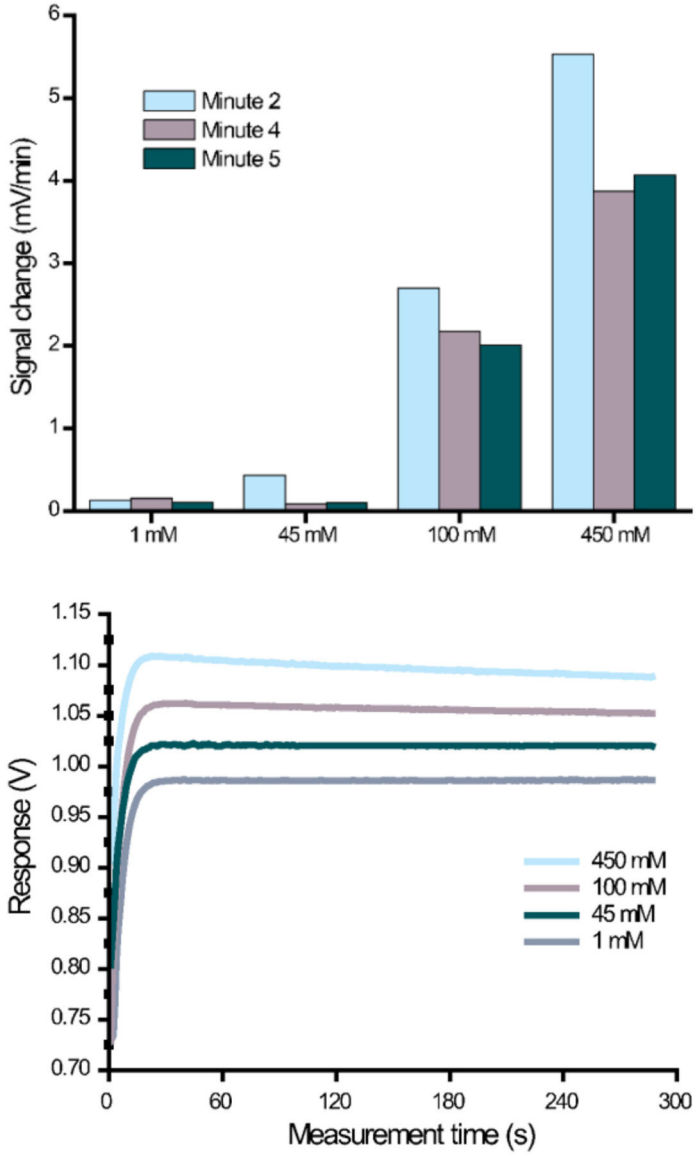

Fig. 4.

(top) Signal drift calculated for four different HS^- concentrations from 60 to 120 s (Minute 2), 180–240 s (Minute 4) and 240–300 s (Minute 5). (bottom) Measurement signals recorded from the time the sensor was powered on.

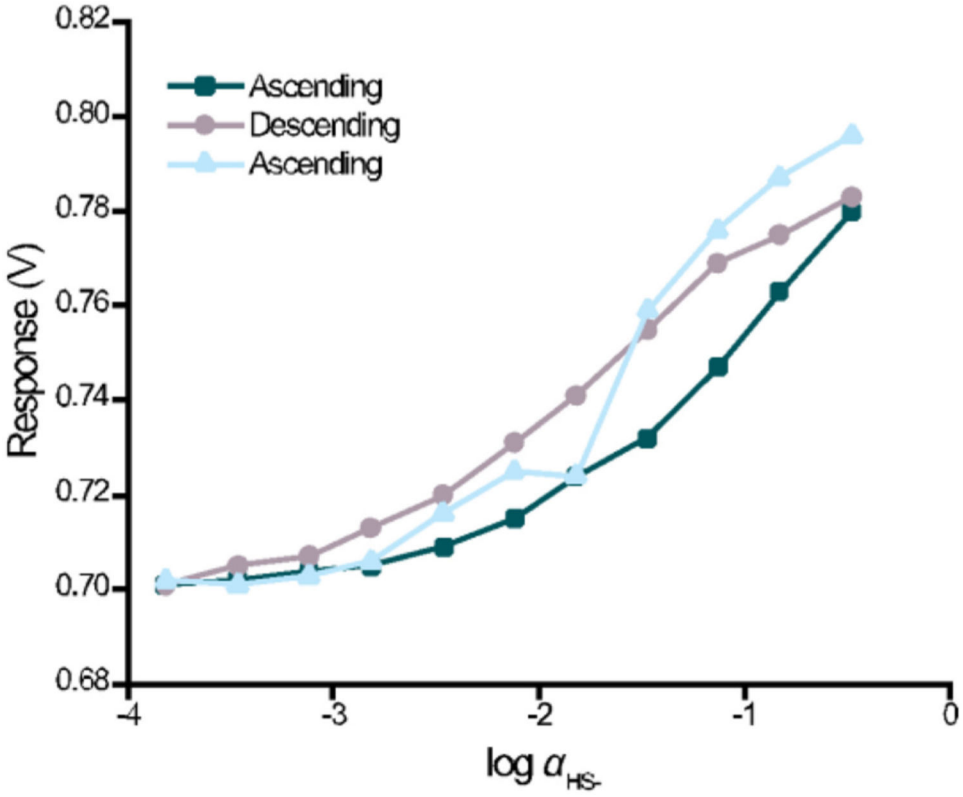

Fig. 5.

Reproducibility of three consecutive calibration experiments for hydrosulfide at pH 8 in the 50 mM PIPES buffer.

Table 1

Summary of selectivity studies performed with TOA/NBR ChemFETs showing selectivity coefficients, effective detection limits (EDL), and corresponding standard error (SEM). All interferents were present at a background level of 200 mM.

Interferent (*X*)	**Selectivity Coefficient ($K_{SH,X}$)**	**EDL (mM)**
Chloride	0.12 ± 0.02	22 ± 2
L-Cysteine	0.13 ± 0.04	20 ± 8
GSH	0.070 ± 0.01	11 ± 2